Supplementary Information

Gated Luminescence Imaging of Silicon Nanoparticles

Jinmyoung Joo,[†] Xiangyou Liu,[‡] Venkata Ramana Kotamraju,[‡] Erkki Ruoslahti,[‡,§] Yoonkey Nam,[#] and Michael J. Sailor[†,]*

[†] Department of Chemistry and Biochemistry, University of California, San Diego, La Jolla, CA 92093, USA

[‡] Cancer Research Center, Sanford-Burnham Medical Research Institute, La Jolla, CA 92037, USA

[§] Center for Nanomedicine and Department of Cell, Molecular and Developmental Biology, University of California, Santa Barbara, Santa Barbara, CA 93106-9610, USA

[#] Department of Bio and Brain Engineering, Korea Advanced Institute of Science and Technology (KAIST), Daejeon 305-701, Korea

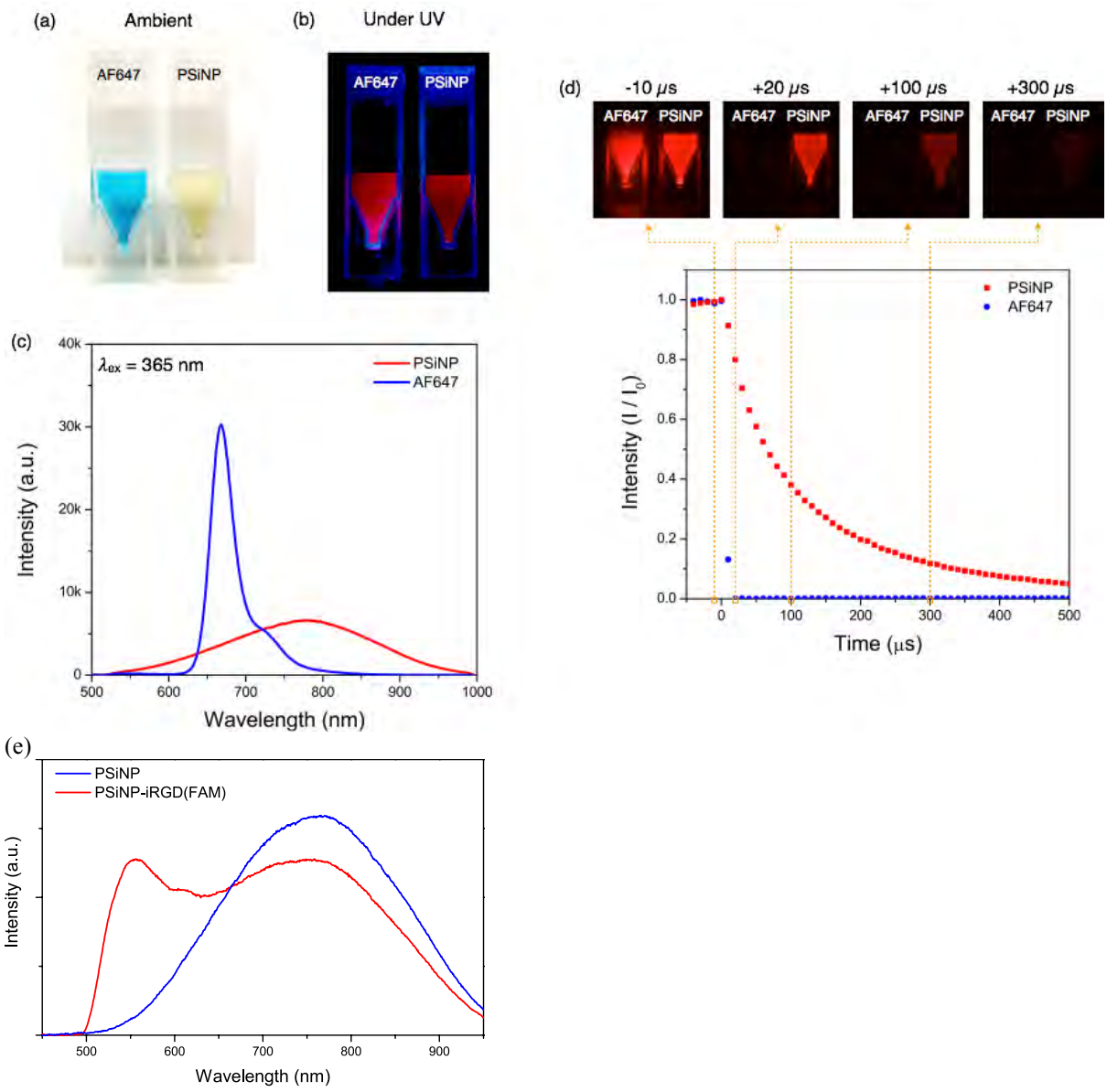

Supplementary Figure S1. Photoluminescence/fluorescence characteristics of PSiNPs and Alexa Fluor (AF647). **(a, b)** Photographs of PSiNP (100 µg/ml) and AF647 (1.5 µg/ml) in deionized water under **(a)** ambient light and **(b)** UV light (λ_{ex} = 365 nm). **(c)** Steady-state luminescence spectra (λ_{ex} = 365 nm, λ_{em} = 460 nm long-pass filter) of PSiNPs and AF647 shown in **(b)**. Integrated intensity between 500 – 1000 nm is 1.97 × 10^6 for AF647 and 2.06 ×10^6 for PSiNP. **(d)** Photoluminescence/fluorescence lifetime decay and corresponding images at each time point. The gate width, gate delay increment step and number of accumulations are 10 µs, 10 µs and 40 times, respectively. Both PSiNPs and AF647 show bright luminescence under continuous excitation, however only PSiNPs show significant luminescence intensity at delayed acquisition times. The time point indicated as 0 µs is the time at which a "turn off" command was sent from the pulse generator to the light source. **(e)** Comparison of steady-state photoluminescence spectra (λ_{ex} = 365 nm) of the PSiNP and PSiNP-iRGD formulations as described in the text. The iRGD peptide contains a fluorescein (FAM) label which appears in the emission spectrum at ~550nm. The FAM label was included in order to estimate its conjugation efficiency to PSiNP-iRGD. FAM-labeling had no substantial effect on the luminescent characteristics (either PL lifetime or λ_{max}) of the PSiNP emission λ_{max} ~ 760 nm.

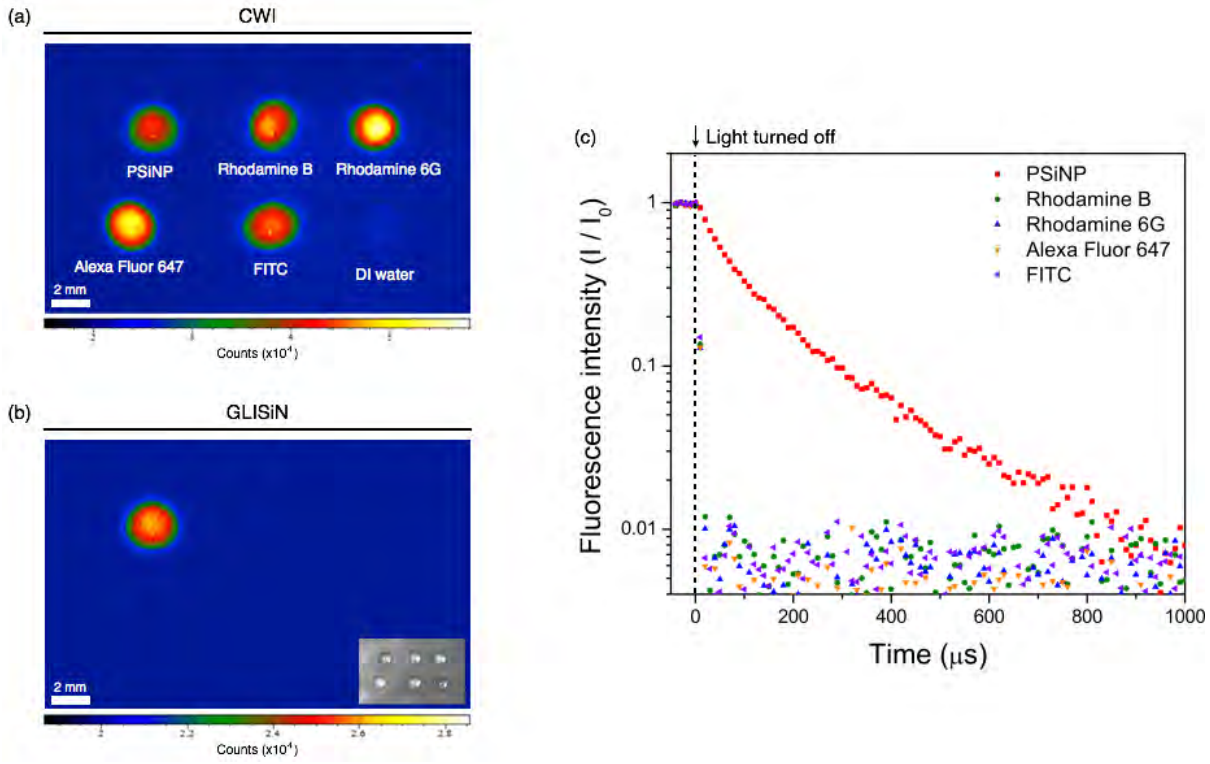

Supplementary Figure S2. Comparison of photoluminescence/fluorescence images of PSiNPs and several standard imaging dyes, in steady-state (**a**, CWI) and time-gated (**b**, GLISiN) imaging modes (λ_{ex} = 365 nm, λ_{em} = 460 nm long-pass filter, gate width: 400 μs, 40 accumulations, gate delay 5 μs). Samples are spotted on black polystyrene plate and intensity is represented in false color with the mapping shown at the bottom of the images. The inset of image (**b**) is a bright field image of the samples obtained under ambient light. The conventional imaging dyes disappear in the GLISiN image (**b**) due to their short-lived emission lifetimes. (**c**) Normalized photoluminescence/fluorescence intensity vs time profiles of each sample, as indicated.

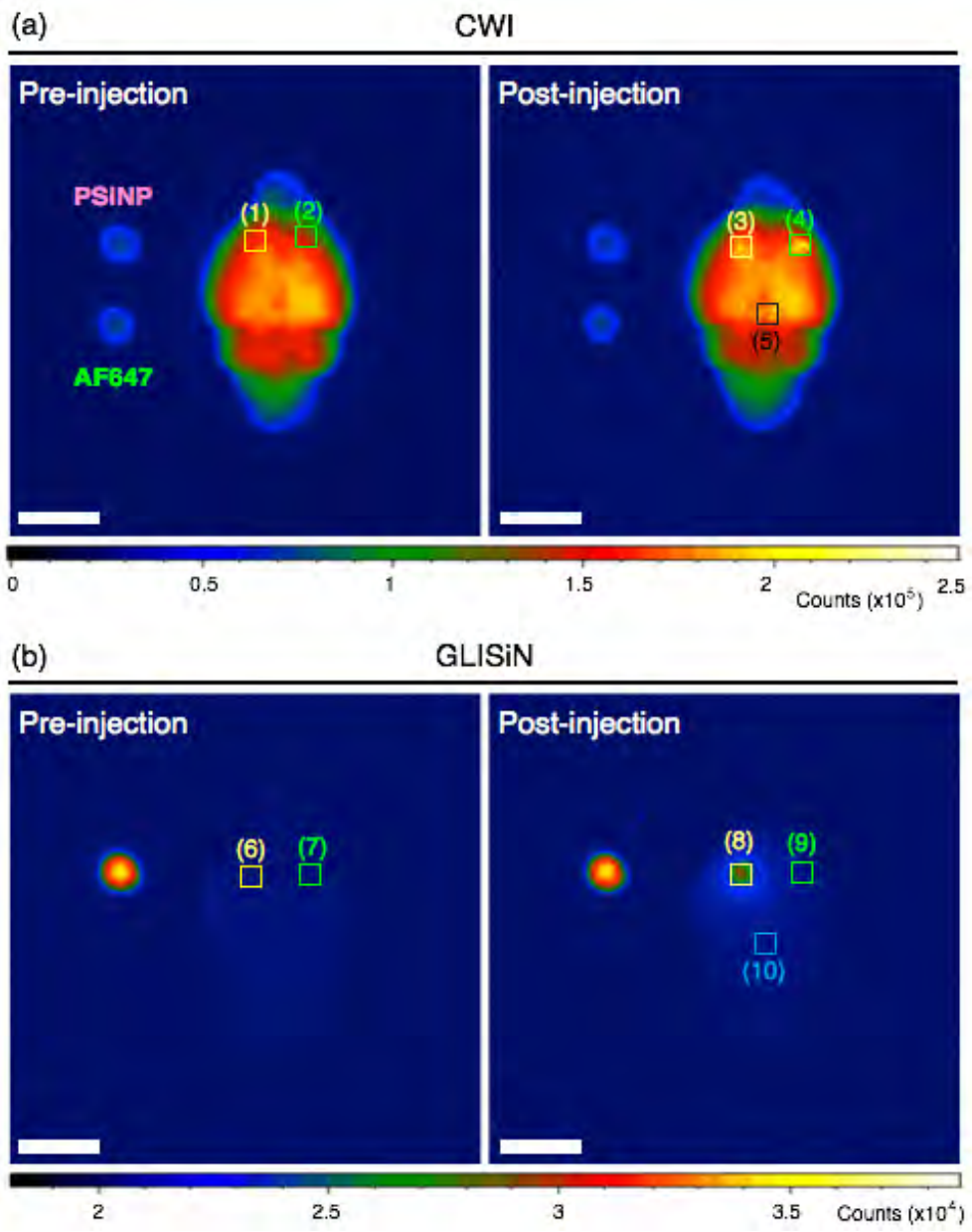

Supplementary Figure S3. *Ex vivo* photoluminescence images of mouse brain before and after local injection of PSiNPs and AF647, corresponding to the samples of **Figure 2** in the manuscript. Each square box shows the region of interest (ROI) for SNR calculation, which is summarized in **Supplementary Table S1**. (a) CW image. (b) GLISiN image. Imaging parameters: λ_{ex}= 365 nm, λ_{em}= 460 nm long-pass filter, gate width: 400 µs, 40 accumulations, gate delay for CW = 0 µs, gate delay for GLISiN = 5 µs. ROI (1), (3), (6), and (8) indicate the PSiNP injection site. ROI (2), (4), (7), and (9) indicate the AF647 injection site. ROI (5) and (10) indicate an adjacent tissue site where no injection was made. Phantom spots of PSiNPs and AF647 made on imaging platform to the left of the organ, as indicated in the first panel of (a).

		vs pre-injection		vs neighboring tissue	
		PSiNPs	AF647	PSiNPs	AF647
CWI	ROI	(3) vs (1)	(4) vs (2)	(3) vs (5)	(4) vs (5)
	SNR	2.19	3.89	0.71	0.85
GLISiN	ROI	(8) vs (6)	(9) vs (7)	(8) vs (10)	(9) vs (10)
	SNR	118	3.21	80.4	0.20
SNR enhancement factor		54.0	-	114	-

Supplementary Table S1. Signal-to-noise ratio (SNR) of photoluminescence signals obtained from the ROIs (signal vs background) shown in **Supplementary Figure S3**. SNR enhancement defined as (SNR of CWI)/(SNR of GLISiN). The column "vs pre-injection" compares the photoluminescence signal obtained from the injected region to the same region measured prior to injection of the indicated imaging agent (PSiNPs or AF647). The column "vs neighboring tissue" compares the photoluminescence signal obtained from the region injected with the indicated imaging agent (PSiNPs or AF647) to a pristine adjacent region of the tissue (where neither imaging agent was injected).

		CWI	GLISiN	SNR enhancement factor
Brain	PSiNP	0.71	80.4	114
	AF647	0.85	0.20	0.24
Liver	PSiNP	1.81	73.0	40.4
	AF647	0.74	2.61	3.54
Heart	PSiNP	3.90	35.1	8.99
	AF647	0.07	0.51	7.04
Kidney	PSiNP	1.22	59.9	49.2
	AF647	0.01	0.05	4.79
Lung	PSiNP	0.31	97.1	312
	AF647	0.72	0.74	1.03
Spleen	PSiNP	4.85	102	20.9
	AF647	10.2	3.28	0.32
Tumor	PSiNP	1.86	48.8	26.3
	AF647	5.33	1.72	0.32

Supplementary Table S2. SNR (vs neighboring tissue) of photoluminescence signals corresponding to **Figure 2d** in the manuscript. Strong tissue autofluorescence overwhelms the photoluminescence/fluorescence signal, thus the SNR is too low to be distinguished from the normal tissue background in most of the CW images (CWI). However, the SNR for the Si nanoparticles is substantial in the GLISiN images of all the organs measured. SNR enhancement factor is defined as the ratio of SNRs of GLISiN vs CWI.

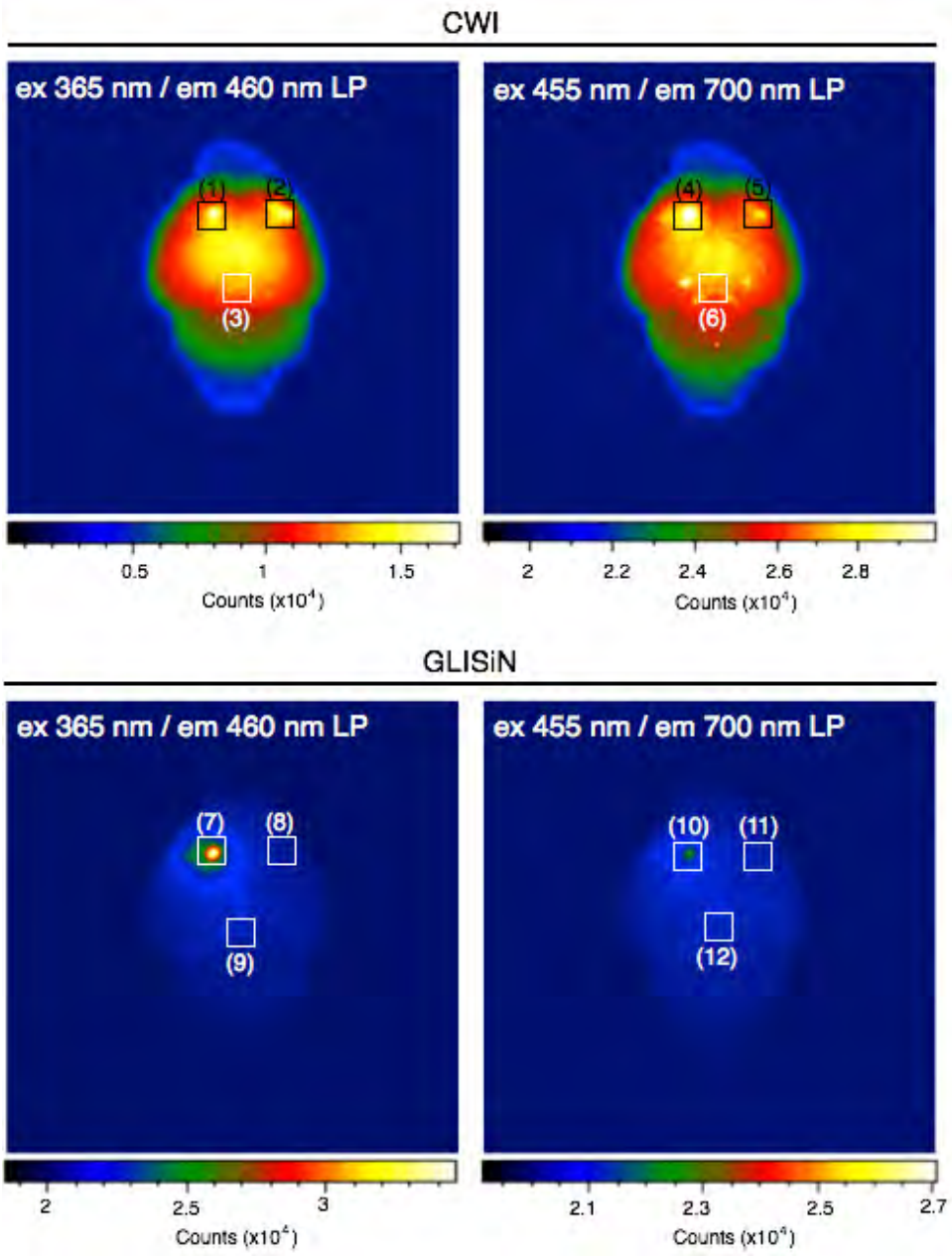

Supplementary Figure S4. *Ex vivo* luminescence images of mouse brain obtained using different excitation/emission bands. Each square box shows the region of interest (ROI) for SNR calculation, which is summarized in **Supplementary Table S3**. 2 µL of PSiNP (150 µg/mL, 300 ng total) and AF647 (10 µg/mL, 20 ng total) were injected directly into the brain tissues.

		Ex 365 nm / Em 460 nm LP		Ex 455 nm / Em 700 nm LP	
		PSiNP	AF647	PSiNP	AF647
CWI	ROI	(1) vs (3)	(2) vs (3)	(4) vs (6)	(5) vs (6)
	SNR	9.73	8.27	13.36	3.80
GLISiN	ROI	(7) vs (9)	(8) vs (9)	(10) vs (12)	(11) vs (12)
	SNR	103	0.14	19.8	0.87
SNR enhancement		10.6	-	1.48	-

Supplementary Table S3. Signal-to-noise ratio (SNR) of photoluminescence/fluorescence signals from the indicated probes (PSiNP or AF647) injected directly in the mouse brain, measured *ex vivo* as indicated in **Supplementary Figure S4**. Noise level is determined from neighboring tissue, and each relevant region of interest (ROI) is as indicated in **Supplementary Figure S4**. "Ex 365 nm / Em 460 nm LP" represents measurements made with 365nm excitation and image captured through a 460nm long pass filter. "Ex 455 nm / Em 700 nm LP" represents measurements made with 455nm excitation and image captured through a 700nm long pass filter. The time-gated method (GLISiN) shows significantly improved SNR under 365 nm excitation (103) but only slight improvement at 455 nm excitation (19.8). The time-gated method (GLISiN) shows better performance under 365 nm excitation relative to 455 nm excitation due to the lower emission quantum yield of PSiNPs when excited at 455 nm.[1]

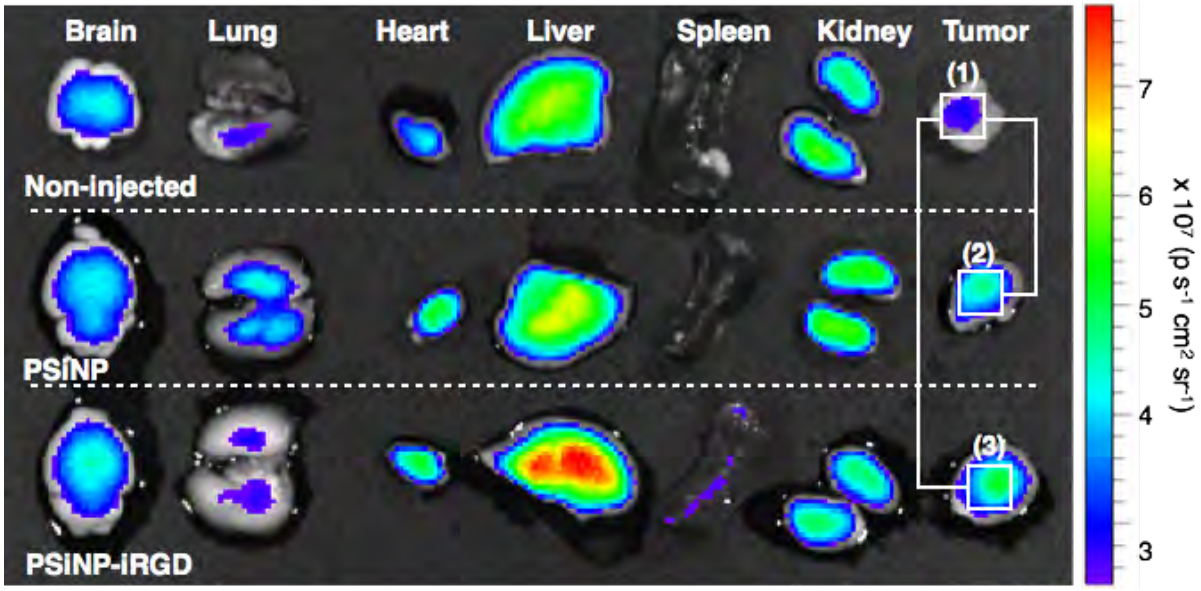

Supplementary Figure S5. *Ex vivo* fluorescence images, using a standard IVIS 200 imaging system, of mouse tissues corresponding to **Figure 3a** in the manuscript. Each white box shows the region of interest (ROI) for the SNR calculation.

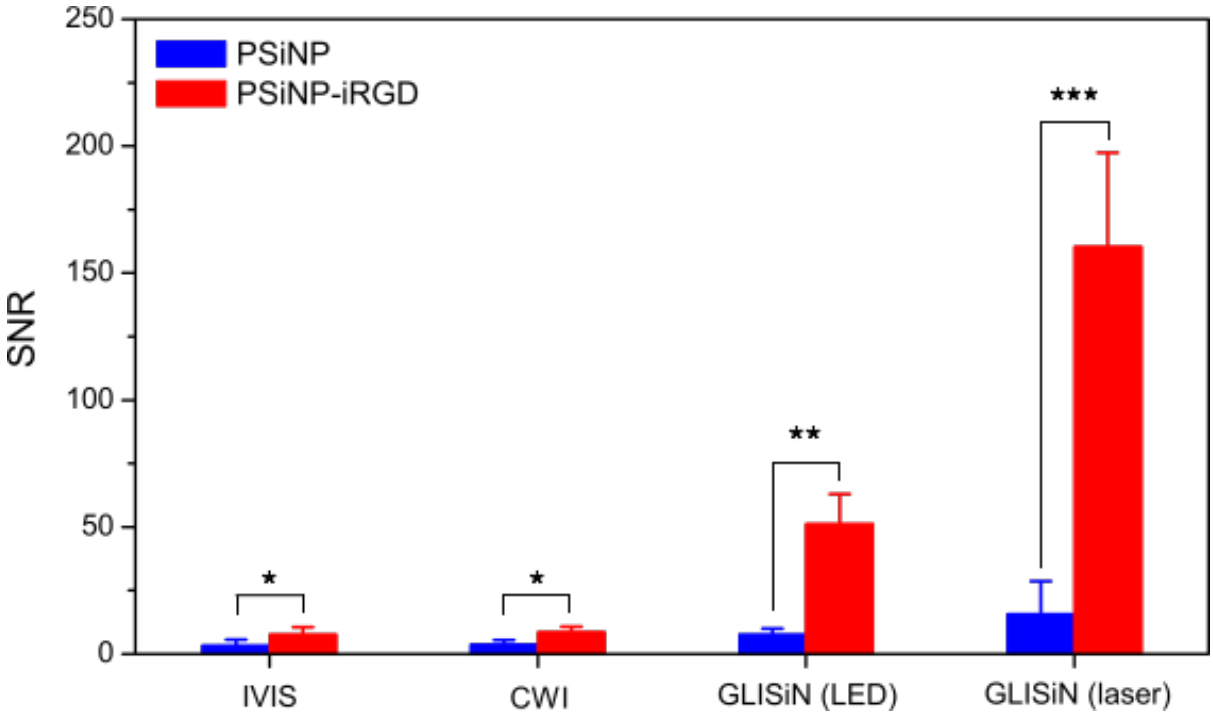

Supplementary Figure S6. Comparison of signal-to-noise ratio (SNR) obtained from measurement of passively accumulated (PSiNP, blue bars) and actively targeted (PSiNP-iRGD, red bars) porous Si nanoparticles in tumor tissues for different imaging modalities. IVIS = commercial IVIS 200 steady-state fluorescence imaging system (λ_{ex}= 445 - 490 nm with GFP filter, λ_{em}= 695-770 nm with Cy5.5 filter); CWI = continuous wave imaging using the same LED and iCCD camera used in the GLISiN images but collected as steady-state images (λ_{ex}= 455 nm, λ_{em}= 700 nm long-pass filter); GLISiN (LED) = Gated Luminescence Imaging of Si Nanoparticles using pulsed UV LED excitation (λ_{ex}= 365 nm, λ_{em}= 460 nm long-pass filter); GLISiN (laser) = image obtained with pulsed laser excitation (λ_{ex}= 455 nm, λ_{em}= 700 nm long-pass filter). Live tumor-bearing mice were injected with untargeted PSiNPs, iRGD-targeted PSiNPs, or phosphate buffered-saline (PBS), and then sacrificed 4 hrs post-injection. SNR is calculated relative to the tumor tissues of PBS-injected mice. The results represent mean ± standard deviation (n=4). Statistical analyses were performed with Student's *t* test (* $p < 0.1$; ** $p < 0.01$; *** $p < 0.005$).

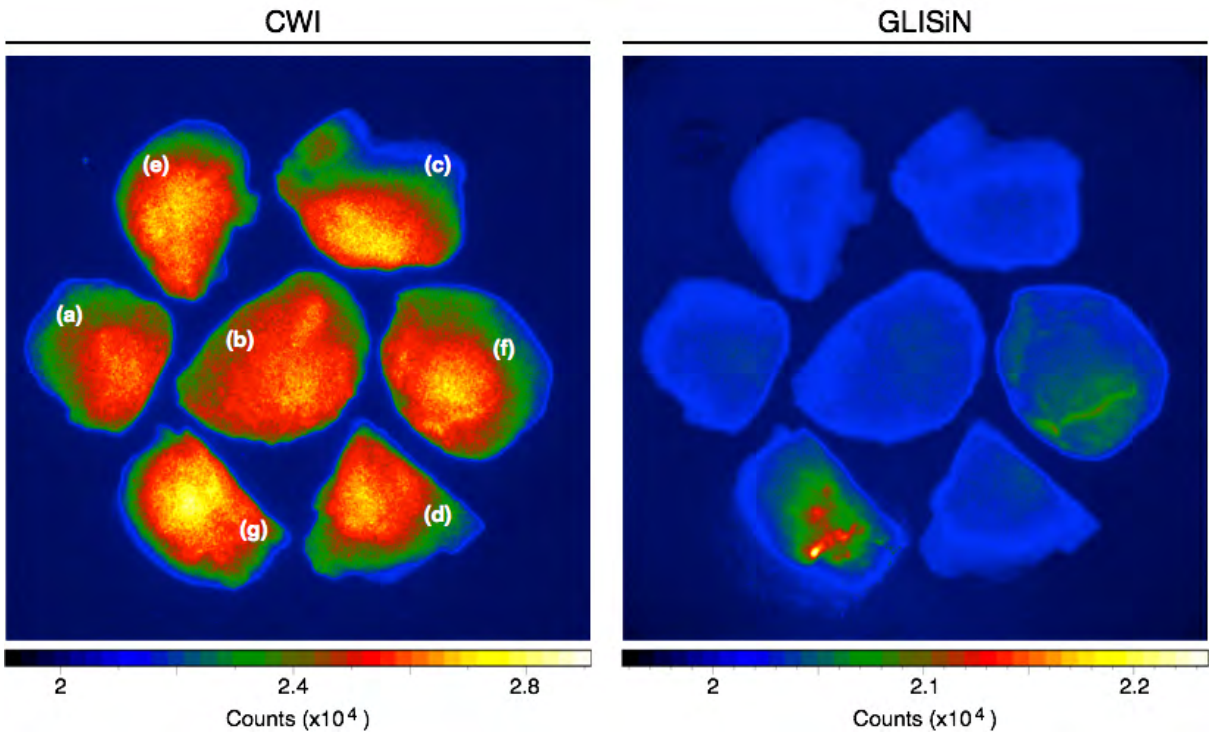

Supplementary Figure S7. Comparison of *ex vivo* photoluminescence images of 4T1 breast tumor tissues harvested from seven different mice, showing the variability of tissue autofluorescence seen in steady-state images (CWI, left image) of tumor sections, and the ability of the GLISiN method (GLISiN, right image) to suppress the high autofluorescence background and more effectively identify luminescence from Si nanoparticles in tissue samples. **(a-d)** non-injected control animals, **(e)** PSiNP-injected animal (*in vivo*, 4 hr prior to sacrifice and harvesting of the organs), **(f)** PSiNP-iRGD-injected animal (*in vivo*, 4 hr prior to sacrifice and harvesting of the organs), and **(g)** PSiNPs-injected directly into the tissue *ex vivo*. Imaging parameters: λ_{ex}= 455 nm, λ_{em}= 700 nm long-pass filter, gate width: 400 µs, 40 accumulations, gate delay for CWI = 0 µs, gate delay for GLISiN = 5 µs.

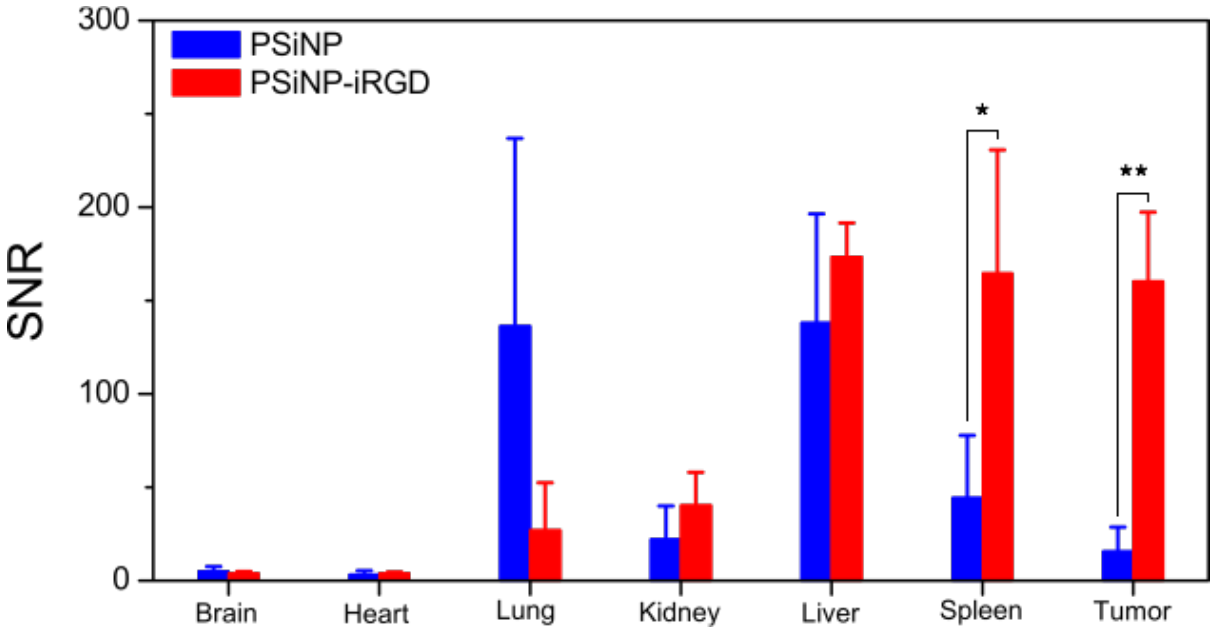

Supplementary Figure S8. Comparison of signal-to-noise ratio (SNR) obtained from measurement of passively accumulated (PSiNP, blue bars) and actively targeted (PSiNP-iRGD, red bars) porous Si nanoparticles in the indicated tissues. Signal-to-noise ratio (SNR) calculated for the nanoparticles accumulated in each organ. Data were obtained using pulsed laser excitation (λ_{ex}= 455 nm, λ_{em}= 700 nm long-pass filter). The SNR is calculated relative to the tissues of PBS-injected mice. The results represent mean ± standard deviation (n=4). Statistical analyses were performed with Student's *t* test (* $p < 0.05$; ** $p < 0.005$). Note that PSiNPs show apparently high uptake in lung in some animals, but the mean value is not significant ($p > 0.1$). It is possible that accumulation of the silicon nanoparticles by the mononuclear phagocyte system (MPS) at reticular connective tissues in the lungs could be responsible for higher uptake seen in some of the animals.[2-4] The size and zeta potential of PSiNP and PSiNP-iRGD are not substantially different (Supplementary Figure S9).

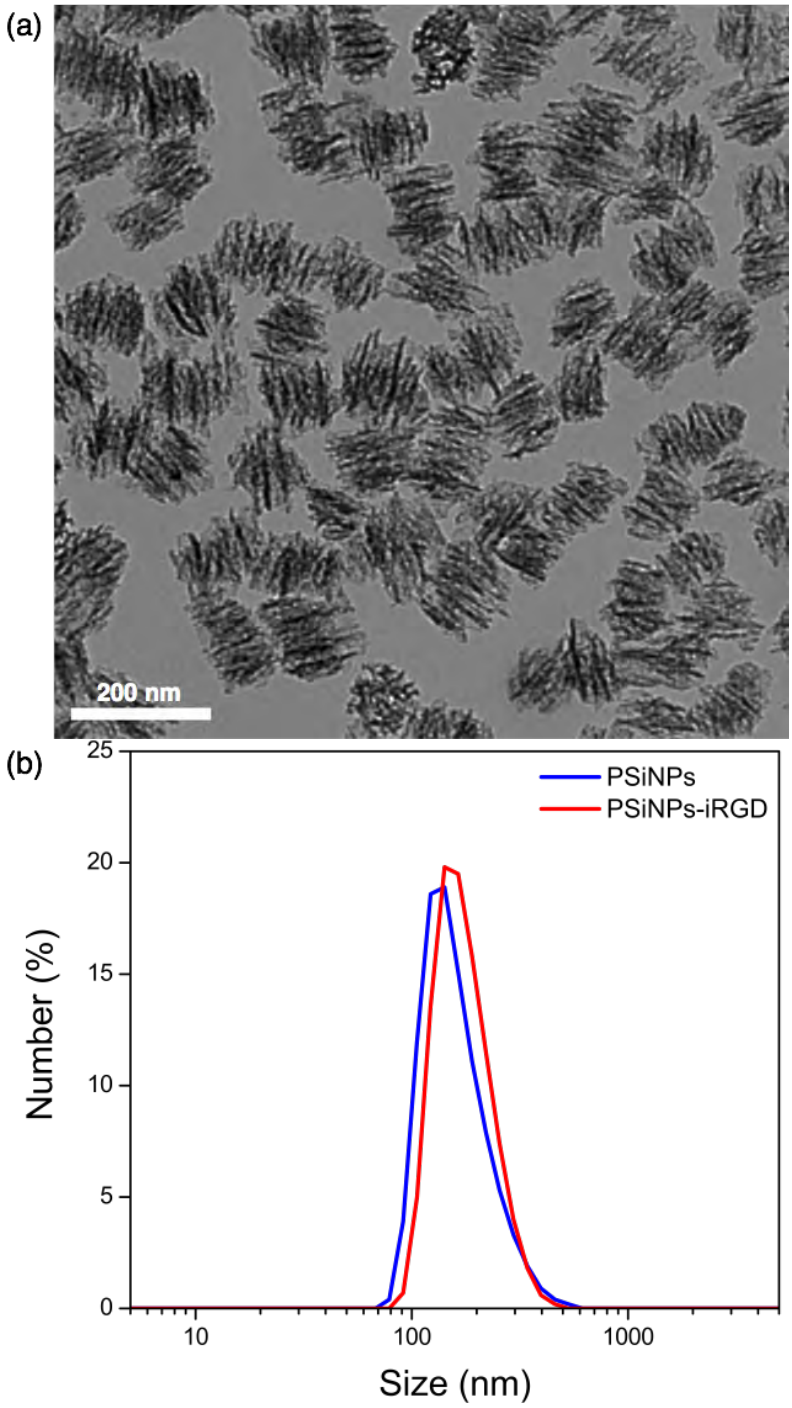

Supplementary Figure S9. (a) Transmission electron microscope image of PSiNPs. (b) Size distribution of PSiNPs obtained from dynamic light scattering (DLS) measurement. Mean diameter of the PSiNP and PSiNP-iRGD formulations are 166 nm and 178 nm, respectively. Measured zeta potential of PSiNP and PSiNP-iRGD is 6.76 mV and 11.53 mV, respectively. Both nanoparticle types were grafted with polyethylene glycol (PEG, Mw. 5000) to prevent nonspecific binding, and they were observed to stably disperse in aqueous solution.

Supplementary Note S1: Discussion on the signal-to-background ratio (SNR)

In this note, we describe the method used to determine the signal-to-noise ratio (SNR) associated with detected photon counts in the region of interest (ROI) of an image. The SNR (or signal-to-background ratio, SBR) is typically defined as the power ratio between a signal (meaningful information) and the background noise (unwanted signal). An alternative definition of SNR is commonly used in image processing, *i.e.*, the ratio of the mean pixel value to the standard deviation of the pixel over a given neighborhood:[5-6]

$$SNR = \frac{\mu_{sig}}{\sigma_{bg}}$$

where μ_{sig} is the signal mean and σ_{bg} is the standard deviation of the noise. Note that the signal mean (μ_{sig}) is the actual signal value relative to the background noise value (**Supplementary Fig. S10b**), so we define the SNR as follows:

$$SNR = \frac{Mean_{sig} - Mean_{bg}}{\sigma_{bg}}$$

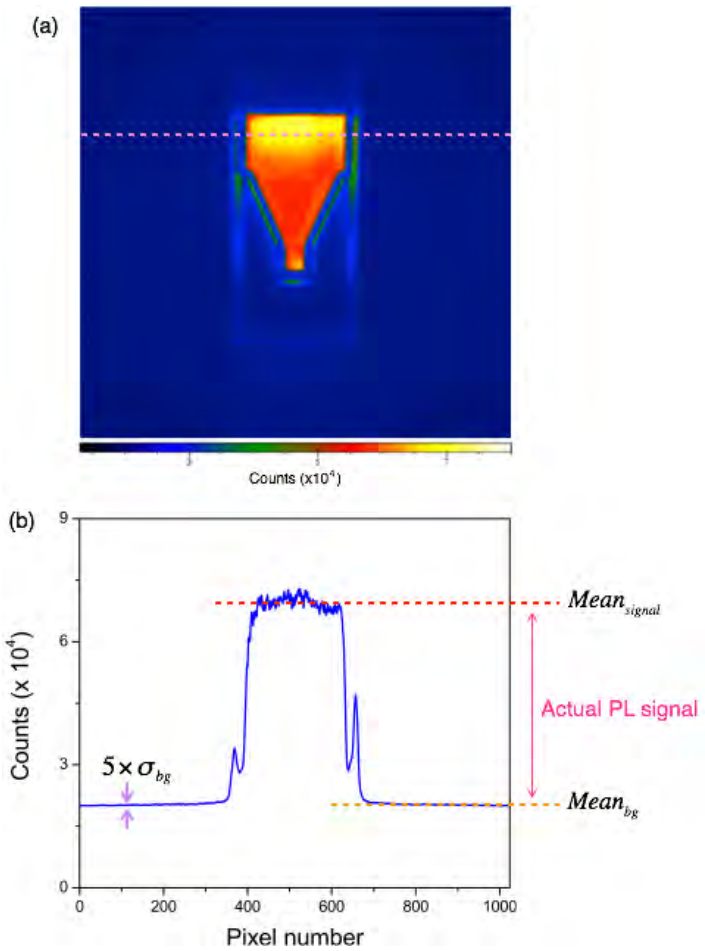

Supplementary Figure S10. (a) Photoluminescence image of PSiNPs in cuvette acquired by the intensified CCD coupled to a macro camera lens, and (b) corresponding intensity plot of the cross section marked in (a).

The SNR is one of the most meaningful metrics that describes the conspicuity of an object. The Rose criterion states that a signal is readily detectable above its background noise at 100% certainty if the SNR is greater than 5, while the detection performance continuously degrades as SNR approaches zero.[6]

Here the $Mean_{sig}$ is the mean intensity of a ROI in the target area, and the $Mean_{bg}$ is from a ROI in the background. The noise can be obtained from the background ROI as well (σ_{bg}). The Andor SOLIS operating software was used for all data acquisition.

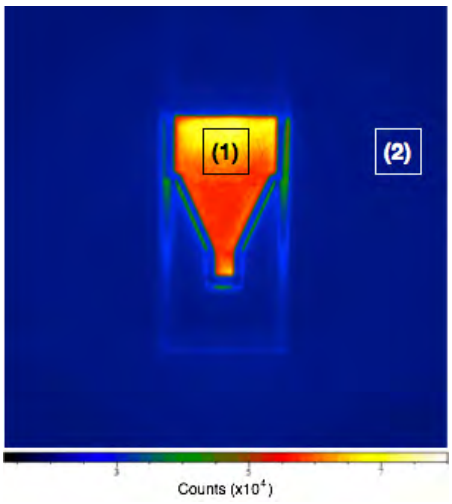

Supplementary Figure S11. Photoluminescence image of PSiNP marked with the region of interest. The $Mean_{sig}$ is obtained in ROI(1), and $Mean_{bg}$ is from ROI(2).

For example in **Supplementary Figure S11**, the SNR of the photoluminescence signal from PSiNP contained in ROI(1) over the background in ROI(2) is calculated as follows:

$$SNR = \frac{Mean_{sig} - Mean_{bg}}{\sigma_{bg}} = \frac{65567 - 20211}{77} = 591$$

Since the photoluminescence intensity is approximately proportional to the concentration of PSiNPs, the SNR also displays a linear relationship with concentration of PSiNPs (**Supplementary Figure S12**). From the Rose criterion, the photoluminescence signal is clearly distinguishable only if the SNR is greater than 5. The minimum detectable concentration of PSiNP is 0.4 μg/mL in this example.

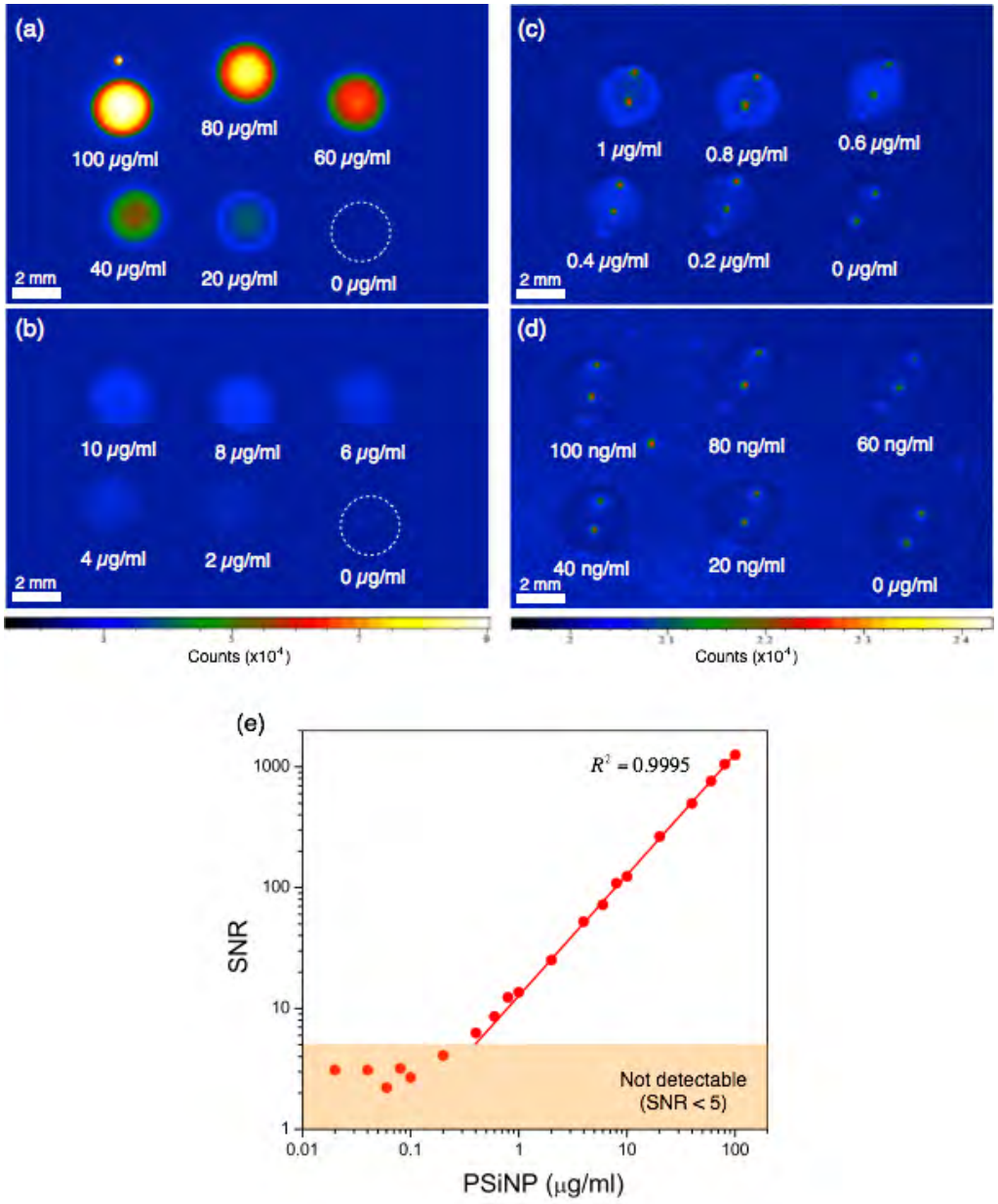

Supplementary Figure S12. (a-d) GLISiN images of PSiNPs (5 µL aliquots) of different concentrations, and **(e)** corresponding SNR of the PSiNP photoluminescence signal over background at each concentration (λ_{ex} = 365 nm, 460 nm long pass filter, gate width: 400 µs, number of accumulations = 40).

Supplementary Note S2: Discussion of GLISiN operating conditions and SNR improvement

The theoretical SNR of PSiNP photoluminescence can increase dramatically with larger gate widths and accumulation times because of the long-lived luminescence signal and the essential absence of detectable signal from short-lived background luminescence at times > 100 ns. In this note, we describe the optimization of GLISiN operating parameters.

As predicted, the SNR substantially increases by extending the gate width (**Supplementary Figure S13**), because the signal mean (μ_{sig}) increases at higher exposure time (longer gate width) while the standard deviation of the noise (σ_{bg}) increases more slowly than the signal mean. Since the luminescence intensity decreases approximately exponentially after the excitation source is switched off and reaches the noise level of the instrumentation after 400 μs ($I/I_0 < 0.07$), the SNR showed very minor improvement for gate widths larger than 400 μs. Therefore, the optimal gate width of 400 μs was used in this study.

In addition, the SNR increases with the number of accumulations due to the higher signal mean (μ_{sig}) with increasing acquisition time, however the standard deviation of the background noise (σ_{bg}) increases more gradually. Although the SNR shows continuous improvement as the number of accumulations increases (**Supplementary Figure S14**), it also increases the time needed to acquire an image (100 ms for single measurement). Here we chose the number of accumulations to be 40, as a compromise between SNR and practical experimental time.

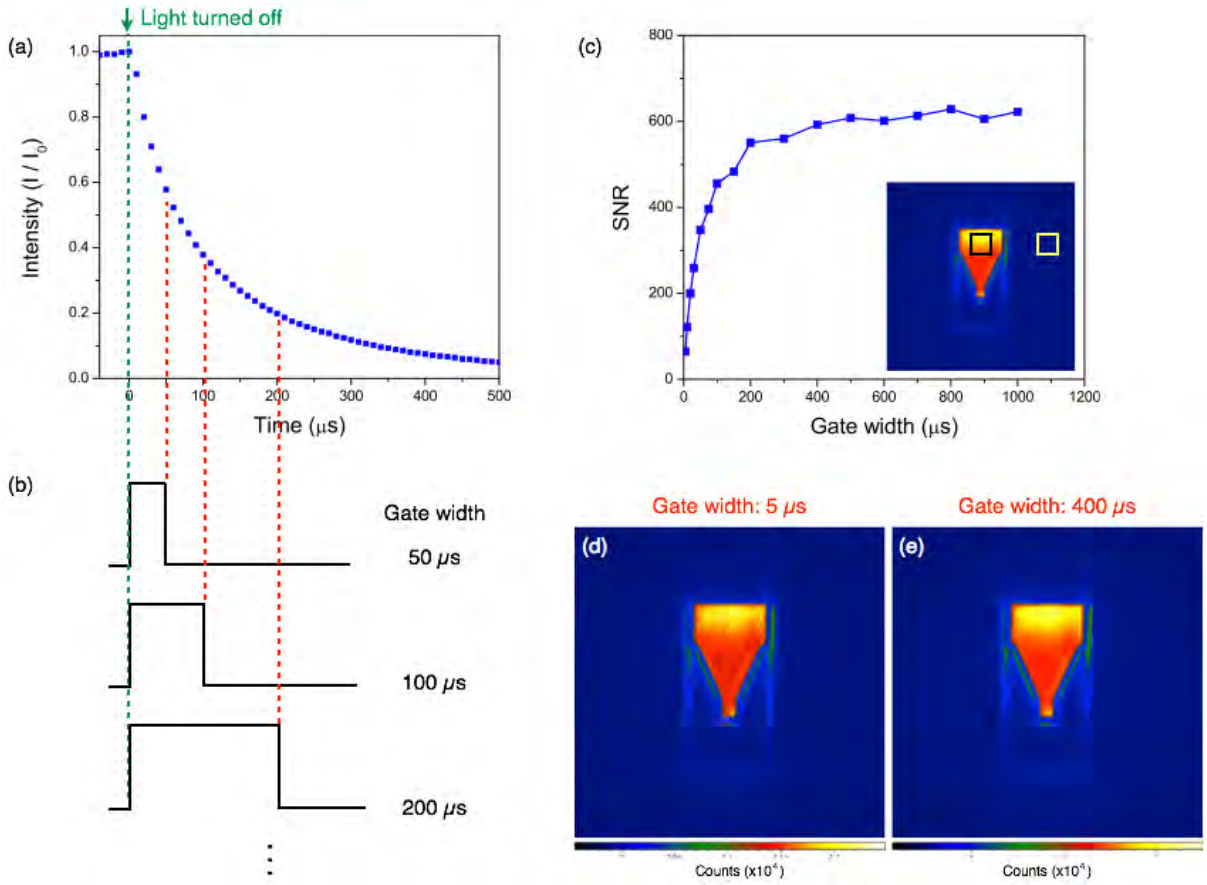

Supplementary Figure S13. Dependence of SNR on gate width used in image acquisition. **(a)** Normalized photoluminescence decay of PSiNPs. **(b)** Schematic of the pulse function indicating the shutter open (image intensifier activated) condition. The Andor operating software externally controls the gate width. **(c)** A plot showing SNR as a function of gate width. In-set: Time-resolved photoluminescence image of PSiNPs in a cuvette (100 µg/mL). Black square indicates the ROI for the signal, and the white square denotes the ROI for background. **(d, e)** GLISiN images of PSiNPs with a gate width of **(d)** 5 µs (SNR: 65) and **(e)** 400 µs (SNR: 592). Number of accumulations = 40.

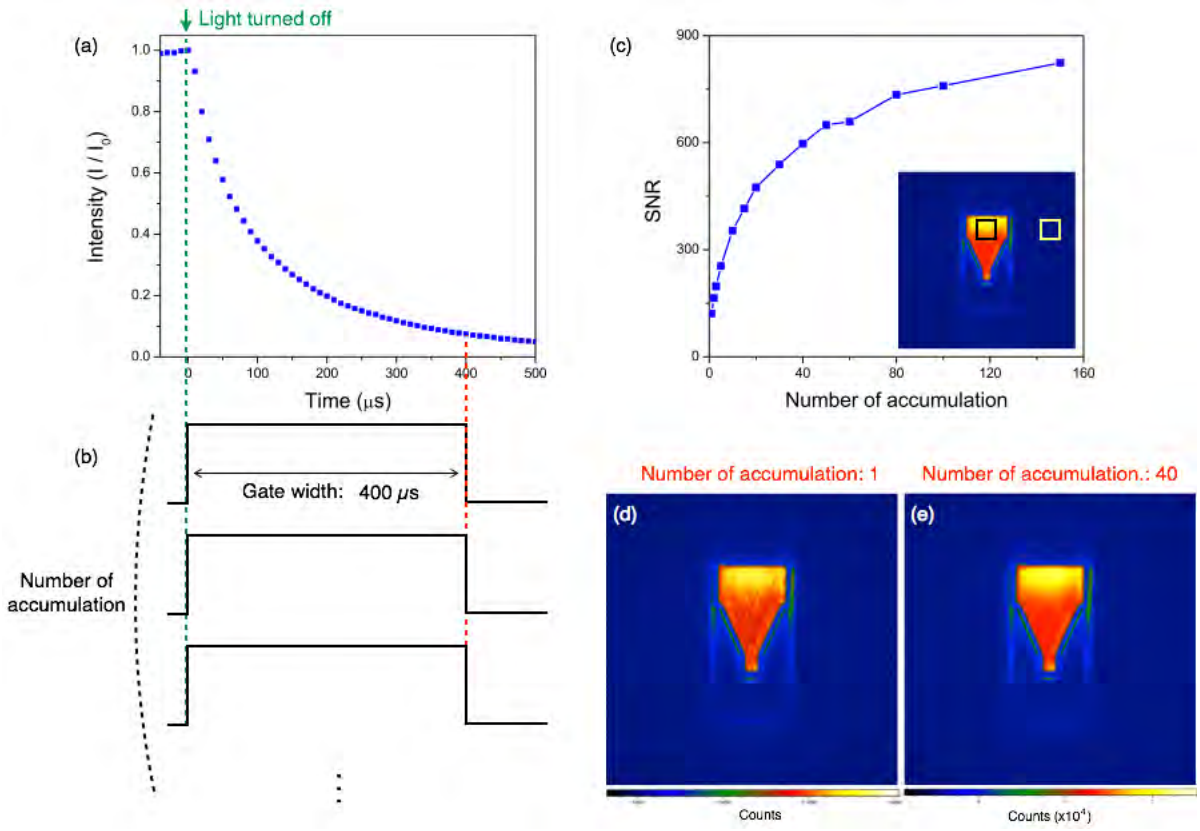

Supplementary Figure S14. Dependence of SNR on the number of accumulations. **(a)** Normalized photoluminescence decay of PSiNPs. **(b)** Schematic of the pulse function indicating the shutter open (image intensifier activated) condition. The gate width is fixed at 400 μs in these experiments. **(c)** A plot showing SNR as a function of accumulation number. In-set: Time-resolved photoluminescence image of PSiNPs (100 μg/mL). Black square is the ROI for signal, and white square is the ROI for background. **(d, e)** GLISiN images of PSiNPs with accumulation number of **(d)** 1 (SNR: 121) and **(e)** 40 (SNR: 597).

References

1. Park, J. H.; Gu, L.; von Maltzahn, G.; Ruoslahti, E.; Bhatia, S. N.; Sailor, M. J., Biodegradable luminescent porous silicon nanoparticles for in vivo applications. *Nat. Mater.* **2009,** *8* (4), 331-336.
2. Anselmo, A. C.; Gupta, V.; Zern, B. J.; Pan, D.; Zakrewsky, M.; Muzykantov, V.; Mitragotri, S., Delivering Nanoparticles to Lungs while Avoiding Liver and Spleen through Adsorption on Red Blood Cells. *ACS Nano* **2013,** *7* (12), 11129-11137.
3. Meng, H.; Xue, M.; Xia, T.; Ji, Z. X.; Tarn, D. Y.; Zink, J. I.; Nel, A. E., Use of Size and a Copolymer Design Feature To Improve the Biodistribution and the Enhanced Permeability and Retention Effect of Doxorubicin-Loaded Mesoporous Silica Nanoparticles in a Murine Xenograft Tumor Model. *ACS Nano* **2011,** *5* (5), 4131-4144.
4. Choi, H. S.; Ashitate, Y.; Lee, J. H.; Kim, S. H.; Matsui, A.; Insin, N.; Bawendi, M. G.; Semmler-Behnke, M.; Frangioni, J. V.; Tsuda, A., Rapid translocation of nanoparticles from the lung airspaces to the body. *Nat. Biotechnol.* **2010,** *28* (12), 1300-U113.
5. Gonzalez, R. C.; Woods, R. E., *Digital image processing*. 3rd ed.; Prentice Hall: Upper Saddle River, N.J., 2008; p xxii, 954 p.
6. Bushberg, J. T., *The essential physics of medical imaging*. 3rd ed.; Wolters Kluwer Health/Lippincott Williams & Wilkins: Philadelphia, 2012; p xii, 1030 p.